Nature. Author manuscript; available in PMC 2014 July 09.

Published in final edited form as:
Nature. 2014 January 9; 505(7482): 234–238. doi:10.1038/nature12815.

Structural basis of lentiviral subversion of a cellular protein degradation pathway

David Schwefel[1], **Harriet C. T. Groom**[2], **Virginie C. Boucherit**[2], **Evangelos Christodoulou**[1], **Philip A. Walker**[1], **Jonathan P. Stoye**[2], **Kate N. Bishop**[2], and **Ian A. Taylor**[1,**]

[1]Division of Molecular Structure, National Institute for Medical Research, The Ridgeway, Mill Hill, London NW7 1AA, UK.

[2]Division of Virology, National Institute for Medical Research, The Ridgeway, Mill Hill, London NW7 1AA, UK.

Abstract

Lentiviruses contain accessory genes that have evolved to counteract the effects of host cellular defence proteins that inhibit productive infection. One such restriction factor, SAMHD1, inhibits HIV-1 infection of myeloid-lineage cells [1,2] as well as resting CD4$^+$ T cells [3,4] by reducing the cellular dNTP concentration to a level where the viral reverse transcriptase cannot function [5,6]. In other lentiviruses, including HIV-2 and related SIVs, SAMHD1 restriction is overcome by the action of viral accessory protein x (Vpx) or the related viral protein r (Vpr) that target and recruit SAMHD1 for proteasomal degradation [7,8]. The molecular mechanism by which these viral proteins are able to usurp the host cell's ubiquitination machinery to destroy the cell's protection against these viruses has not been defined. We present here the crystal structure of a ternary complex of Vpx with the host cell's E3 ligase substrate adaptor DCAF1 and the C-terminal region of SAMHD1. Vpx is made up of a three-helical bundle, stabilised by a zinc finger motif and wraps tightly around the disc-shaped DCAF1 molecule to present a new molecular surface. This adapted surface is then able to recruit SAMHD1 via its C-terminus making it a competent substrate for the E3 ligase to mark for proteasomal degradation. The structure provides the first description of how a lentiviral accessory protein is able to subvert the cell's normal protein degradation pathway to inactivate the cellular viral defence system.

HIV-1 infection of myeloid and CD4+ T cells is inhibited by the post-entry restriction factor SAMHD1. In other primate lentiviruses, including HIV-2 and SIV, this block is overcome by the expression of the Vpx accessory protein. Vpx recruits SAMHD1 to the DDB1/CUL4A/ROC1 E3 ubiquitin ligase complex through interaction with the substrate-adaptor protein DCAF1 and facilitates its degradation through the proteasomal pathway [1,2,7,8]. To understand the mechanism of Vpx-mediated recruitment of SAMHD1 we assessed which regions of each molecule (Figure 1a) are required for the interaction. These data reveal that only SAMHD1 molecules containing a C-terminal region (residues 582-626) are able to support ternary complex formation; compare central and left panels (Figure 1b) and that this region alone is sufficient for the interaction, right panel, Figure 1b. We therefore determined

---

**Any correspondence and requests for materials should be addressed to I.A.T. (itaylor@nimr.mrc.ac.uk)..

Author Contributions: D.S., H.C.T.G., V.C.B., E.C. and P.A.W performed experiments. D.S., H.C.T.G., V.C.B., E.C., P.A.W., J.P.S., K.N.B. and I.A.T. contributed to experimental design, data analysis and manuscript writing.

The coordinates of DCAF1-CtD/Vpx$_{sm}$/SAMHD1-CtD have been deposited in the Protein Data Bank under accession number 4CC9.

The authors declare no competing financial interests.

Europe PMC Funders Author Manuscripts

the crystal structure of the ternary complex of the C-terminal WD40 domain of DCAF1 (DCAF1-CtD) together with the Vpx of SIV from Sooty mangabey (Vpx_{sm}) and the C-terminal region of SAMHD1 (SAMHD1-CtD). The crystal structure was solved by SAD (**Extended Data Figure 1, Table 1**) and is shown in Figure 1c. DCAF1-CtD comprises a seven-bladed β-propeller disc-shaped molecule 45 Å in diameter and 20 Å in depth. Vpx_{sm} comprises an antiparallel V-shaped 3-helical bundle that wraps around one side and the top of DCAF1-CtD. This arrangement of helices is conserved in the HIV-1 Vpr solution structure [9]. However, the structures differ significantly at the helical termini and in Vpx_{sm} zinc coordinated by $His39V_{pxsm}$, $His82V_{pxsm}$, $Cys87_{Vpxsm}$ and $Cys89_{Vpxsm}$ (Figure 1c, 2a) brings together the C-termini of helices-1 and 3 to stabilise the structure. Residues Asn606 to Asp624 of SAMHD1-CtD are also well ordered. They form two short perpendicular α-helices, helix-A (Leu610-Ala613) and helix-B (Arg617-Lys622) connected by a three-residue linker (S614-S616) and pack into a cleft between Vpx_{sm} and DCAF1-CtD (Figure 1c).

The complex contains four interfacial regions (Figure 2b), a combined Vpx_{sm}/SAMHD1/DCAF1 ternary interface (Figure 2c) and a more extensive DCAF1/Vpx_{sm} binding surface with three sites of interaction (Figure 2d-f). The Vpx_{sm}/SAMHD1 interaction buries 700 $Å^2$ of molecular surface. At the interface the hydrophobic side chains of Leu610, Val618, Leu620 and Phe621 from SAMHD1 helix-A and -B pack into a hydrophobic pocket between the amino-termini of Vpx_{sm} helix-1 and -3 (Figure 2c). The interface also contains electrostatic interactions between acidic residues $Glu15_{Vpxsm}$ and $Glu16_{Vpxsm}$ at the N-terminus of Vpx_{sm} helix-1 and Arg609 and Arg617 part of a tri-basic Arg609/Arg617/Lys622 motif in SAMHD1. By contrast, the contact area between SAMHD1-CtD and DCAF1-CtD is small, just 210$Å^2$. The only direct interaction is between Lys622 in the SAMHD1 tri-basic motif and Asp1092 of DCAF1 in the acidic Glu1091-Asp-Glu1093 loop connecting blade-7 and -1 of the DCAF1-CtD propeller (Figure 2c). Asp1092 is also hydrogen-bonded to $Tyr66_{Vpxsm}$ in an interaction that bridges SAMHD1-CtD and Vpx_{sm}. Several other key residues in Vpx_{sm} also mediate bridging interactions. These include $Trp24_{Vpxsm}$ that stacks against Arg617 of SAMHD1-CtD as well as hydrogen bonding to DCAF1 - Asn1135 (Figure 2e) and $Tyr69_{Vpxsm}$ that packs with Val618 of SAMHD1-CtD and is also hydrogen-bonded to the side chain of Glu1091 in the DCAF1-CtD Glu-Asp-Glu loop.

The DCAF1/Vpx_{sm} interface is much larger, made up from three sites of interaction burying 2000 Å of surface (Figure 2d-f, **Extended Data Table 2**). The first involves the N-terminal extended region of Vpx_{sm} ($Glu6_{Vpxsm}$ - $Ser13_{Vpxsm}$) that packs against the concave surface of DCAF1 blade-1 spanning from the underside to the topside of the disc, making several hydrogen bonds and hydrophobic interactions (Figure 2d). Further interactions involve $Trp24_{Vpxsm}$, $Thr28_{Vpxsm}$, $Ile32_{Vpxsm}$ and $Gln76_{Vpxsm}$ in helix-1 and -3 that contact residues on the DCAF1-CtD blade-1 and -2 and the interspersing loop (Figure 2e). Helix-3 of Vpx_{sm} lies in a groove between blade-1 and -7 on the upper face of DCAF1-CtD. Interactions between the charged and hydrophobic side chains of $Lys77_{Vpxsm}$, $Arg70_{Vpxsm}$, $Phe80_{Vpxsm}$ and $Met81_{Vpxsm}$ along its length with residues in the intra-strand loops of blade-1 and -7 of DCAF-CtD including the Glu-Asp-Glu loop comprise the third region of the DCAF1/Vpx interface (Figure 2f).

Mutation of many of the residues at these interfaces have been shown previously to reduce viral infectivity, disrupt Vpx binding to DCAF1 and interfere with proteasomal degradation of SAMHD1 (**Extended Data Table 3**). Examples include: the bridging residue, $Trp24_{vpxsm}$ [10] (Figure 2c, e), $Gln76_{Vpxsm}$ [11] that is hydrogen bonded to Asn1135 and Trp1156 of DCAF1 (Figure 2e) and $Lys77_{Vpxsm}$ [12] that is integral to an extensive salt bridge

network that links residues in the DCAF1 Glu-Asp-Glu loop with $Arg70_{Vpxsm}$, $Tyr69_{Vpxsm}$ and $Tyr66_{Vpxsm}$ in helix-3 of Vpx_{sm} (Figure 2f).

In the structure, SAMHD1-CtD makes salt bridges at both the Vpx_{sm} and DCAF1-CtD interfaces through charged side chains in the tribasic motif. *In vitro* binding studies show that full length SAMHD1 and SAMHD1-CtD have comparable affinity for the DDB1/Vpx/DCAF1 complex [13]. However, to test if SAMHD1-CtD alone is sufficient for recruitment by Vpx and to assess the contribution of the tri-basic motif, an *in vivo* reporter assay was employed. SAMHD1-CtD was fused to the C-terminus of a tandem NLS-GFP protein that localises to the nucleus [14]. 293T Cells transduced with the NLS-GFP-SAMHD1-CtD fusion, (Figure 3a) display GFP fluorescence in their nuclei (Figure 3b). Delivery of Vpx by infection with a SIV-(Vpx^+) virus, greatly reduces the number of GFP^+ cells, (Figure 3b, c). By contrast, infection with a SIV-(Vpx^-) virus or addition of the proteasomal inhibitor MG132 with Vpx^+ virus does not reduce the population of GFP^+ cells (Figure 3b, c), indicating that loss of GFP fluorescence results from Vpx-mediated proteasomal degradation of NLS-GFP-SAMHD1-CtD. In addition, mutation of residues in the SAMHD1 tribasic motif (Arg609/Arg617/Lys622) to alanine or glutamate also abolishes or severely diminishes the capacity of Vpx to induce degradation of NLS-GFP-SAMHD1-CtD (Figure 3b, c). These data reveal that SAMHD1-CtD in isolation acts as a Vpx-dependent degron to induce the proteasomal turnover of a heterologous protein and that disruption of the protein-protein interactions observed in the crystal structure prevent Vpx-mediated degradation. When the same mutations are introduced into SAMHD1 they also reduce the capacity of Vpx to induce degradation, albeit to varying degrees (Figure 3d). However, all display wildtype restriction of HIV-1 indicating that the CtD is not required for SAMHD1 anti-HIV-1 activity (Figure 3e).

To put the DCAF1-CtD/Vpx_{sm}/SAMHD1-CtD structure into the context of the E3 ligase a molecular model of the entire CUL4A/DDB1/ROC1/DCAF/SAMHD1/Vpx_{sm} assembly was constructed by superposition of DCAF1-CtD/Vpx_{sm}/SAMHD1-CtD onto existing structures in the PDB database. First, the β-propellers of DCAF1-CtD and the related substrate adaptor, DDB2 were aligned (**Extended Data Figure 2, inset**) facilitating substitution of DCAF1-CtD for DDB2 in the existing DDB1-DDB2 structure [15]. The DDB1-CUL4A/ROC1 interface is highly flexible [16]. Therefore, the DCAF1-CtD/Vpx_{sm}/SAMHD1-CtD/DDB1 model was superposed onto the two most extreme conformations available allowing the range of orientations that CUL4A/ROC can adopt with respect to Vpx_{sm} and SAMHD1 to be visualised (**Extended Data Figure 2**). The model places Vpx_{sm} and SAMHD1-CtD on the opposite face of the DCAF1-CtD disk from the DCAF1-DDB1 binding site, accessible to the RING domain of ROC1. Moreover, in both conformations SAMHD1 is placed in the proximity of the ROC1 RING domain, ideally located for ubiquitin transfer. Notably, regions of SAMHD1 proximal to the bound SAMHD-CtD are required for catalytic activation/tetramerisation [17] and association with Vpx/DCAF1/DDB1 inhibits SAMHD1 catalysis [13] suggesting that recruitment to the CUL4A/DDB1/ROC1 complex might additionally down-regulate SAMHD1 activity thorough tetramer disassembly.

Reprogramming of the CUL4/DDB1//ROC1 E3 ubiquitin ligase is also employed by paramyxovirus and hepatitis B Virus (HBV) to subvert the cellular antiviral response. These viruses usurp the interaction of DDB1 with DCAF1 by installing the viral substrate recruitment factors V or X in its place [18,19]. In lentiviruses, a different strategy has evolved where the substrate recruitment factor, DCAF1, is itself adapted by association with accessory proteins to create a new binding pocket, in the case of Vpx_{sm} and Vpx_{HIV-2} to recruit SAMHD1 through its C-terminal region (**Extended Data Figure 3**). Notably, the SAMHD1 tribasic motif is conserved amongst primates but is absent in species that are not HIV/SIV hosts (Figure 4a). Similarly, the N-terminal Vpx_{sm} sequence $_9$PPGNSGEET$_{17}$

containing $Glu15_{Vpxsm}$ and $Glu16_{Vpxsm}$ that make salt bridges with Arg609 and Arg617 is conserved amongst all Vpx proteins that target human SAMHD1 for degradation (Figure 4b) [7] suggesting that the complementarity between these motifs is a driver of the specificity of the SAMHD1-CtD/Vpx interaction. In Vpx proteins that do not induce degradation of human SAMHD1[7,20], red-capped Mangabey (Vpx_{rcm}) and Mandrill (Vpx_{mnd2}), $_{9}PPGNSGEET_{17}$ is not conserved, (Figure 4b). However, these Vpx proteins still induce degradation of SAMHD1 but do so by targeting it to DCAF1 through sequences located toward the N-terminus of [20].

In some SIVs, the evolutionally related accessory protein Vpr recruits SAMHD1 for degradation [7]. By contrast, Vpr_{HIV-1} still associates with DCAF1 and the CUL4A/DDB1/ROC1 E3 ligase but results in cell cycle arrest at G2, likely through recruitment of an unidentified cellular factor to the E3 [21-23]. In the complex, we identified a structural zinc binding-site in Vpx_{sm} (Figure 2a) that is conserved in both Vpx and Vpr proteins (Figure 4b). Mutation of His71 in Vpr_{HIV-1}, the equivalent of the Vpx_{sm} zinc-coordinating His82, abrogates DDB1-DCAF1 binding and Vpr-induced cell cycle arrest [24]. Furthermore, most of the other conserved residues map to the DCAF1 interface (Figure 4c) and mutation of two of these ($Gln65_{Vpr}$ and $Trp18_{Vpr}$, the equivalents of $Gln76_{Vpx}$ and $Trp24_{Vpx}$) also results in loss of Vpr function [23,25] (**Extended Data Table 3**). These observations now suggest a strong structural conservation between these related accessory proteins. Moreover, given that Vpr-induced cell cycle arrest is also mediated through association with DCAF1 and the actions of the CUL4A/DDB1/ROC1 E3 [21-23] it is likely that both factors utilise a similar mechanism to target cellular proteins to the CUL4A complex (**Extended Data Figure 3**). Consequently, although the cellular target(s) of Vpr are unknown the ternary complex presented here provides a structural model for the design of therapeutic agents that target the Vpx− and Vpr-DCAF1 interaction.

METHODS

Cloning, protein expression and purification

The DNA sequence coding for human SAMHD1 residues Q582-M626 (SAMHD1-CtD) was amplified by PCR from cDNA template using the oligonucleotide primer sequences: forward – ggc GGATCC t cag gat ggc gat gtt ata gcc cc, reverse - ggc GCGGCCGC tca tca cat tgg gtc atc ttt aaa aag ctg g. The PCR product was gel-purified and ligated into the pET52b plasmid (Merck Millipore) using standard restriction enzyme cloning to generate an N-terminal Strep-II-tagged fusion protein. N-terminally GST-tagged Sooty mangabey Vpx residues M1-A112 (Vpx_{sm}) in the pET49b plasmid (Merck Millipore) was a generous gift of Dr David Goldstone (University of Auckland). Human DCAF1 residues A1058-E1396 (DCAF1-CtD) were amplified by PCR from cDNA template using the oligonucleotide primer sequences: forward - ggc CCATGG ca tca ttt cca aag tat gga ggg g, reverse - ggc GAGCTC ctc tgc cag acg ctg cct gcc. The PCR product was gel-purified and ligated into the pTriEx-6 plasmid (Merck Millipore) using standard restriction enzyme cloning to generate a C-terminal 10xHis-tagged fusion protein. Insert sequences were verified by DNA sequencing.

SAMHD1-CtD and GST-Vpx_{sm} were expressed in the *E. coli* strain Rosetta 2 (DE3) (Merck Millipore). Bacterial cultures were grown in an incubator shaker at 37 °C. Protein expression was induced by the addition of 0.1 mM IPTG at A_{600} = 0.5. Afterwards, cultures were cooled to 18 °C and grown for further 20 h. To produce seleno-methionine (SeMet) -labelled Vpx_{sm}, cells were grown to A_{600} = 0.5 at 37°C in M9 minimal medium. Then, an amino acid supplement (L-lysine, L-phenylalanine, L-threonine to a final concentration of 100 mg/l, L-isoleucine, L-leucine, L-valine and L-SeMet to a final concentration of 40 mg/l, respectively) was added to inhibit endogenous methionine biosynthesis and start SeMet

incorporation [26]. Fifteen minutes after addition, the culture was cooled to 18 °C. Protein expression was induced by the addition of 0.5 mM IPTG, and cells were grown for further 20 h.

Cultures were centrifuged for 20 min at 4,500 xg and 4 °C. Cell pellets were resuspended in 30 ml lysis buffer (50 mM Tris-Hcl pH 7.8, 500 mM NaCl, 4 mM $MgCl_2$, 0.5 mM TCEP, 1x EDTA-free mini complete protease inhibitors (Roche), 0.1 U/ml Benzonase (Novagen) per pellet of 1 L bacteria culture. Cells were lysed in an EmulsiFlex-C5 (Avestin). The lysate was cleared by centrifugation for 1 h at 48,000 xg and 4 °C. All further purification steps were performed at 4 °C or on ice. The cleared lysates were applied to 10 ml StrepTactin (IBA, for SAMHD1-CtD) or to 10 ml Glutathione-Sepharose (GE Healthcare, for GST-Vpx_{sm}) columns. Columns were washed with 600 ml wash buffer (50 mM Tris-HCl pH 7.8, 500 mM NaCl, 4 mM $MgCl_2$, 0.5 mM TCEP). Column-immobilized GST-Vpx_{sm} was additionally washed with 250 ml of wash buffer supplemented with 5 mM ATP, followed by 250 ml wash buffer supplemented with 1% CHAPS. SAMHD1-CtD was eluted from the column with 25 mM ammonium bicarbonate pH 7.5, 2.5 mM desthiobiotin. The elution peak was lyophilized, resuspended in 500 μl of 25 mM ammonium bicarbonate pH 7.5 and applied to a Superdex75 16/60 gel filtration column (GE Healthcare) equilibrated with 25 mM ammonium bicarbonate pH 7.5. The peak fractions were pooled, lyophilized and resuspended in 10 mM Bis-tris propane pH 8.5, 150 mM NaCl, 4 mM $MgCl_2$, 0.5 mM TCEP. Small aliquots at a concentration of approximately 2 mM were flash-frozen in liquid nitrogen and stored at −80 °C. GST-Vpx_{sm} was eluted from the column with wash buffer supplemented with 20 mM glutathione. The elution peak was concentrated to 5 ml and incubated overnight with 1 mg GST-3C protease. Cleaved Vpx_{sm} was further purified on a Superdex200 26/60 gel filtration column (GE Healthcare) equilibrated with 10 mM Tris-HCl pH 7.8, 150 mM NaCl, 4 mM $MgCl_2$, 0.5 mM TCEP. Peak fractions containing Vpx_{sm} were concentrated to approximately 20 mg/ml and flash-frozen in liquid nitrogen in small aliquots for further storage at −80 °C. Seleno-methionine-substituted Vpx_{sm} was purified in the same way.

For the production of DCAF1-CtD, recombinant baculovirus was generated by cotransfecting *Sf9* cells with pTriEx-DCAF1-CtD and linearised $BAC10{:}1629_{KO}$ [27]. *Sf9* cells were cultured in SF900 II serum free medium (Invitrogen) at 28 °C. In a typical preparation, 2 L of *Sf9* cells at 2×10^6 cells/ml density were infected with 4 ml of high titre DCAF1-CtD virus for 48h. For structure determination, selenium was incorporated into DCAF1-CtD by supplementing 921 Δ series medium (Expression Systems, LLC) with 50 mg/l seleno-methionine.

Sf9 cultures were centrifuged for 20 min at 4500x g and 4°C. Pellets were resuspended in 30 ml lysis buffer (50 mM Tris-HCl pH 7.8, 500 mM NaCl, 4 mM $MgCl_2$, 30 mM imidazole-HCl pH 7.8, 0.5 mM TCEP, 1x EDTA-free mini complete protease inhibitors (Roche), 0.1 U/ml Benzonase (Novagen)) per pellet of 1 L culture. Cells were lysed in an EmulsiFlex-C5 (Avestin). The lysate was cleared by centrifugation for 1 h at 48,000 xg and 4 °C. All further purification steps were performed at 4 °C or on ice. The cleared lysate was applied to a 1 ml Ni-NTA Sepharose column (GE Healthcare). The column was washed with 500 ml wash buffer (50 mM Tris-HCl pH 7.8, 500 mM NaCl, 4 mM $MgCl_2$, 30 mM imidazole-HCl pH 7.8, 0.5 mM TCEP). Protein was eluted with wash buffer supplemented with 300 mM imidazole pH 7.8. Peak fractions were pooled, concentrated to 2 ml and applied on a Superdex200 16/60 gel filtration column (GE Healthcare) equilibrated with 10 mM Tris-HCl pH 7.8, 150 mM NaCl, 4 mM $MgCl_2$, 0.5 mM TCEP. Peak fractions containing DCAF1-CtD were pooled, concentrated to approximately 20 mg/ml and flash-frozen in liquid nitrogen in small aliquots for further storage at −80°C. Seleno-methionine-substituted DCAF1-CtD was purified in the same way.

Assembly of the ternary complex

Initially, the complex was prepared by mixing 100 μg of DCAF1-CtD, Vpx_{sm} and SAMHD1-CtD in 10 mM Bis-tris propane pH 8.5, 150 mM NaCl, 4 mM $MgCl_2$, 0.5 mM TCEP, followed by incubation overnight on ice. Complex formation was assessed by applying the mixture on an analytical Superdex75 10 300 GL gel filtration column (GE Healthcare), equilibrated with 10 mM Bis-tris propane pH 8.5, 150 mM NaCl, 4 mM $MgCl_2$, 0.5 mM TCEP and SDS-PAGE analysis (Molecular weight of markers 97, 66.3, 55.4, 36.5, 31.0, 21.5, 14.4, 6.0 and 3.5 kDa). After optimisation, for large scale preparation of the complex, DCAF1-CtD, Vpx_{sm} and SAMHD1-CtD were mixed in a molar ratio of 1:1.5:1.5 in 0.1 M Bis-tris propane pH 8.5, 150 mM NaCl, 4 mM $MgCl_2$, 0.5 mM TCEP and incubated overnight on ice. The mixture was applied to a Superdex 75 16/60 gel filtration column (GE Healthcare) equilibrated with 10 mM Bis-tris propane pH 8.5, 150 mM NaCl, 4 mM $MgCl_2$, 0.5 mM TCEP. Peak fractions containing all components were pooled, concentrated to approximately 5 mg/ml and directly used for crystallization experiments, after addition of an equimolar amount of SAMHD1-CtD.

Crystallisation and structure determination

The native DCAF1-CtD-Vpx_{sm}-SAMHD1-CtD complex was crystallised by vapour diffusion using an Oryx crystallisation robot (Douglas Instruments). Crystals were obtained from 0.1 μl droplets containing an equal volume of 2.5 mg/ml protein complex in 10 mM Bis-tris propane pH 8.5, 150 mM NaCl, 4 mM $MgCl_2$, 0.5 mM TCEP mixed with 0.2 M magnesium chloride, 0.1 M Hepes pH 7.5, 15% PEG 400. For data collection, crystals were adjusted to 25 % PEG 400 and cryo-cooled in liquid nitrogen. Native crystals diffracted up to 2.5 Å resolution on beamline I03 at the Diamond Light Source, UK and belong to the space group $P2_12_12_1$ with cell dimensions of a=73.79, b=82.03, c=113.29 with a single copy of the complex in the asymmetric unit. Crystals of the complex containing seleno-methionine-substituted DCAF1-CtD and Vpx_{sm} were grown using the vapour diffusion method by mixing 1 μl complex at 5 mg/ml with 1 μl reservoir solution containing 0.4 M magnesium sulphate, 0.1 M MES pH 6.5. Crystals were adjusted to 25 % glycerol and cryo-cooled in liquid nitrogen. A SAD dataset was collected on beamline I04 at the Diamond Light Source, UK at a wavelength of 0.97972 Å, corresponding to the anomalous f″ peak wavelength for selenium determined from an X-ray fluorescence scan. The crystal diffracted up to 3.5 Å resolution and was nearly isomorphous to the native crystal with the same space group and unit cell dimensions of a=74.25, b=82.88, c=115.56. Data were reduced using the XDS suite [28]. An initial set of 5 selenium sites was found using the programs SHELXC and SHELXD [29]. These sites were used as input for the program autoSHARP [30], which added 2 more sites and performed density modification, leading to an interpretable electron density map. A nearly complete model for Vpx_{sm} and a partial polyalanine trace of DCAF1-CtD were located in this initial map using the buccaneer chain-tracing program [31]. Completion of the polyalanine trace of DCAF1-CtD and placement of the protein backbone of SAMHD1-CtD was then undertaken manually in Coot [32]. A round of refinement against native data recorded to 2.5Å produced an improved map that allowed further building of the SAMHD1-CtD and DCAF1-CtD side-chains. Subsequent incorporation of a Zn^{2+} ion and ligands in Coot combined with positional, real-space, individual B-factor and TLS refinement in phenix.refine [33] produced a final model for residues 1073-1314, 1328-1392 of DCAF1-CtD, 5-90, 100-111 of Vpx_{sm} and 606-624 of SAMHD1-CtD with R-/R_{free}-factors of 17.8 %/21.6 %. In the model, 97.1 % of residues have backbone dihedral angles in the favoured region of the Ramachandran plot, 2.66 % fall in the allowed regions and 0.24 % are outliers. Details of data collection and refinement statistics are presented in **Extended Data Table 1**.

Multiple sequence alignment

Amino acid sequences were aligned using the ClustalW server and adjusted manually. Abbreviations and Uniprot ID, SAMHD1: Hs-*Homo sapiens* Q9Y3Z3, Pt-*Pan troglodytes* H6WE97, Ca-*Cercocebus atys* H6WEA6, Ct-*Cercocebus torquatus* H6WEA7, Mam-*Macaca mulatta* F7CA64, Cj-*Callithrix jacchus* F7IGP7, Cf-*Canis familiaris* E2QTR2, Mum-*Mus musculus* Q60710, Rn-*Rattus norvegicus* D3Z898, Gg- *Gallus gallus* Q5ZJL9, Xl-*Xenopus laevis* Q6INN8, Dr-*Danio rerio* Q502K2, Dd- *Dictyostelium discoideum* B0G107. Vpx: sm-sooty mangabey (*Cercocebus atys*) P19508, mac-rhesus macaque (*Macaca mulatta*) P05917, rcm-red-capped mangabey (*Cercocebus torquatus*) NCBI GenBank HM803689, mnd-mandrill (*Mandrillus sphinx*) NCBI Reference Sequence NP_758889, HIV-2A P06939, HIV-2B Q89721. Vpr: HIV-2A P06938, HIV-2B P0C1P6, HIV-1MA P05955, HIV-1MB P35967

Modelling of the cullin/RING ubiquitin ligase assembly

Structural superposition was carried out using SSM [34] implemented in PDBefold (http://www.ebi.ac.uk/msd-srv/ssm/). DCAF1-CtD was first superposed with the DDB2 β-propeller in the DDB1-DDB2 structure (PDB code 3EI3) such that the N-terminal residues and first β-strand of DCAF1-CtD align with equivalent sequence just C-terminal to the helical DDB1-binding element of DDB2, termed the H-box. The second β-propeller domain of DDB1 (BPB), which serves as anchor for the CUL4 scaffold (wheat half-transparent surface), is mobile with respect to the DDB1 BPA and BPC. The two most extreme BPB conformations available in the PDB database were used to model the rotational range of the CUL4 arm with respect to DDB1-BPB (PDB codes 2HYE, to the left and 3I7H, to the right).

Restriction assay

SAMHD1 wildtype sequence was inserted into pLGatewayIeYFP [35] and mutations created by PCR-based site directed mutagenesis. MoMLV-based YFP vectors were made by cotransfecting pVSV-G [36], pKB4 [37] and pLgatewaySN_SAMHD1 (wildtype or mutants) into 293T cells, harvesting 48 h post-transfection. HIV-1GFP was made as above by cotransfecting pVSV-G, p8.91 [38] and pCSGW [39]. U937 cells [40] were maintained in RPMI + [L]Glutamine (GIBCO) with 10 % fetal calf serum (biosera), penicillin and streptomycin. Cells (1×10^6) were transduced by spinoculation at 1,700 rpm for 90 min with 0.5 ml neat virus in the presence of 1 μg/ml polybrene. Cells were differentiated by addition of 100 nM phorbol myristate acetate for 72 hr and infected with HIV-1GFP. Restriction was assessed by 2-colour flow cytometry after 72 hr.

Transfection and immunoblotting

SAMHD1 and HIV-2 Vpx sequences were amplified from pLgatewaySN_SAMHD1 and pIRES2-EGFP-Vpx (gift from Mario Stevenson) respectively and cloned into pCMS28 [41]. Point mutations were created by PCR-based site directed mutagenesis. 293T cells were cotransfected with 2 μg each pCMS28-SAMHD1 and -Vpx, wild type, mutant proteins or empty vector. Cells were harvested 24 h post-transfection and analysed by SDS PAGE followed by immunoblotting with anti-SAMHD1 3295 (generated in house), anti-HIV-2 Vpx (hybridoma 6D2.6 supernatant, NIH AIDS Reagent Program 2739) and anti-14-3-3 (C-16, Santa Cruz sc-731).

Degron assay

A reporter construct comprising two copies of green fluorescent protein with a N-terminal nuclear localisation signal (NLS) fused to residues 600-626 of SAMHD1 was synthesised (GenArt, NLS-GFP-SAMHD1-CtD, Figure 3a). NLS-GFP-SAMHD1-CtD was inserted into pCMS28 using BglII and EcoRI. All mutants were created by PCR-based site directed

mutagenesis. Puromycin virus-like particles were generated by co-transfection of pVSVG, pKB4 and pCMS28-NLS-GFP-SAMHD1-CtD wildtype or mutant as above. The stable cell lines were made by transduction of 293T cells followed by puromycin selection. VLPs SIV Vpx+ and Vpx− were generated by co-transfection of pVSVG and a SIV Gag-Pol expression plasmid pSIV3+ [42] or pSIV3+$_{vpx-}$ (gift from Caroline Goujon and Andreas Cimarelli). Viral titres were quantified using a modified ELISA for reverse transcriptase activity (Cavidi). 293T cells stably expressing SAMHD1-GFP wildtype or mutant were seeded at 5×10^4 cells per well in a 24-well plate one day prior to infection. Cells were infected with 2-fold serial dilutions of replication defective SIV Vpx+ virus in the presence of 1 μg/ml polybrene. For each experiment, SIV Vpx− VLPs and proteasome inhibitor MG132 (25.2 μM) were included as negative controls. After 48 hours, cells were harvested and the percentage of GFP-positive cells was determined by flow cytometry using a FACSVerse analyser (BD Biosciences). In parallel, GFP expression was analysed by microscopy using an inverted fluorescent microscope (LEICA).

Supplementary Material

Refer to Web version on PubMed Central for supplementary material.

Acknowledgments

We thank Lesley Haire and Roksana Ogrodowicz for help with crystallisation, Prof. Ian Jones (Reading University) for the provision of the modified *A. californica* baculovirus bacmid, BAC10: 1629KO, Steve Smerdon and Steve Gamblin for comments on the manuscript. We gratefully acknowledge Diamond Light Source for synchrotron access (Grant No. 7707). This work was supported by the UK Medical Research Council, file references U117565647 (I.A.T) U117592729 (K.N.B) U117512710 (J.P.S), the Wellcome Trust, ref. 084955 (K.N.B) and by an EMBO long-term fellowship co-funded by the European Commission Marie Curie Actions (EMBOCOFUND2010, GA-2010-267146) (D.S).

References

1. Laguette N, et al. SAMHD1 is the dendritic- and myeloid-cell-specific HIV-1 restriction factor counteracted by Vpx. Nature. 2011; 474:654–657. doi: 10.1038/nature10117. pii: nature10117. [PubMed: 21613998]
2. Hrecka K, et al. Vpx relieves inhibition of HIV-1 infection of macrophages mediated by the SAMHD1 protein. Nature. 2011; 474:658–661. doi:10.1038/nature10195. [PubMed: 21720370]
3. Baldauf HM, et al. SAMHD1 restricts HIV-1 infection in resting CD4(+) T cells. Nature medicine. 2012; 18:1682–1687. doi:10.1038/nm.2964.
4. Descours B, et al. SAMHD1 restricts HIV-1 reverse transcription in quiescent CD4(+) T-cells. Retrovirology. 2012; 9:87. doi:10.1186/1742-4690-9-87. [PubMed: 23092122]
5. Goldstone DC, et al. HIV-1 restriction factor SAMHD1 is a deoxynucleoside triphosphate triphosphohydrolase. Nature. 2011; 480:379–382. doi: 10.1038/nature10623. pii: nature10623. [PubMed: 22056990]
6. Lahouassa H, et al. SAMHD1 restricts the replication of human immunodeficiency virus type 1 by depleting the intracellular pool of deoxynucleoside triphosphates. Nature immunology. 2012; 13:223–228. doi:10.1038/ni.2236. [PubMed: 22327569]
7. Lim ES, et al. The ability of primate lentiviruses to degrade the monocyte restriction factor SAMHD1 preceded the birth of the viral accessory protein Vpx. Cell host & microbe. 2012; 11:194–204. doi: 10.1016/j.chom.2012.01.004. [PubMed: 22284954]
8. Ahn J, et al. HIV/simian immunodeficiency virus (SIV) accessory virulence factor Vpx loads the host cell restriction factor SAMHD1 onto the E3 ubiquitin ligase complex CRL4DCAF1. The Journal of biological chemistry. 2012; 287:12550–12558. doi:10.1074/jbc.M112.340711. [PubMed: 22362772]
9. Morellet N, Bouaziz S, Petitjean P, Roques BP. NMR structure of the HIV-1 regulatory protein VPR. Journal of molecular biology. 2003; 327:215–227. [PubMed: 12614620]

10. Wei W, et al. A novel DCAF1-binding motif required for Vpx-mediated degradation of nuclear SAMHD1 and Vpr-induced G2 arrest. Cellular microbiology. 2012; 14:1745–1756. doi:10.1111/j.1462-5822.2012.01835.x. [PubMed: 22776683]
11. Srivastava S, et al. Lentiviral Vpx accessory factor targets VprBP/DCAF1 substrate adaptor for cullin 4 E3 ubiquitin ligase to enable macrophage infection. PLoS Pathog. 2008; 4:e1000059. doi: 10.1371/journal.ppat.1000059. [PubMed: 18464893]
12. Bergamaschi A, et al. The human immunodeficiency virus type 2 Vpx protein usurps the CUL4A-DDB1 DCAF1 ubiquitin ligase to overcome a postentry block in macrophage infection. J Virol. 2009; 83:4854–4860. doi: 10.1128/JVI.00187-09. pii: JVI.00187-09. [PubMed: 19264781]
13. DeLucia M, Mehrens J, Wu Y, Ahn J. HIV-2 and SIVmac accessory virulence factor Vpx down-regulates SAMHD1 enzyme catalysis prior to proteasome-dependent degradation. The Journal of biological chemistry. 2013; 288:19116–19126. doi:10.1074/jbc.M113.469007. [PubMed: 23677995]
14. Bennett EJ, Bence NF, Jayakumar R, Kopito RR. Global impairment of the ubiquitin-proteasome system by nuclear or cytoplasmic protein aggregates precedes inclusion body formation. Molecular cell. 2005; 17:351–365. doi:10.1016/j.molcel.2004.12.021. [PubMed: 15694337]
15. Scrima A, et al. Structural basis of UV DNA-damage recognition by the DDB1-DDB2 complex. Cell. 2008; 135:1213–1223. doi:10.1016/j.cell.2008.10.045. [PubMed: 19109893]
16. Fischer ES, et al. The molecular basis of CRL4DDB2/CSA ubiquitin ligase architecture, targeting, and activation. Cell. 2011; 147:1024–1039. doi:10.1016/j.cell.2011.10.035. [PubMed: 22118460]
17. Yan J, et al. Tetramerization of SAMHD1 is required for biological activity and inhibition of HIV infection. The Journal of biological chemistry. 2013; 288:10406–10417. doi:10.1074/jbc.M112.443796. [PubMed: 23426366]
18. Angers S, et al. Molecular architecture and assembly of the DDB1-CUL4A ubiquitin ligase machinery. Nature. 2006; 443:590–593. doi:10.1038/nature05175. [PubMed: 16964240]
19. Li T, Robert EI, van Breugel PC, Strubin M, Zheng N. A promiscuous alpha-helical motif anchors viral hijackers and substrate receptors to the CUL4-DDB1 ubiquitin ligase machinery. Nature structural & molecular biology. 2010; 17:105–111. doi:10.1038/nsmb.1719.
20. Fregoso OI, et al. Evolutionary Toggling of Vpx/Vpr Specificity Results in Divergent Recognition of the Restriction Factor SAMHD1. PLoS pathogens. 2013; 9:e1003496. doi:10.1371/journal.ppat.1003496. [PubMed: 23874202]
21. Wen X, Duus KM, Friedrich TD, de Noronha CM. The HIV1 protein Vpr acts to promote G2 cell cycle arrest by engaging a DDB1 and Cullin4A-containing ubiquitin ligase complex using VprBP/DCAF1 as an adaptor. J Biol Chem. 2007; 282:27046–27057. doi: 10.1074/jbc.M703955200. pii: M703955200. [PubMed: 17620334]
22. Schrofelbauer B, Hakata Y, Landau NR. HIV-1 Vpr function is mediated by interaction with the damage-specific DNA-binding protein DDB1. Proceedings of the National Academy of Sciences of the United States of America. 2007; 104:4130–4135. doi:10.1073/pnas.0610167104. [PubMed: 17360488]
23. Le Rouzic E, et al. HIV1 Vpr arrests the cell cycle by recruiting DCAF1/VprBP, a receptor of the Cul4-DDB1 ubiquitin ligase. Cell Cycle. 2007; 6:182–188. pii: 3732. [PubMed: 17314515]
24. Hrecka K, et al. Lentiviral Vpr usurps Cul4-DDB1[VprBP] E3 ubiquitin ligase to modulate cell cycle. Proceedings of the National Academy of Sciences of the United States of America. 2007; 104:11778–11783. doi:10.1073/pnas.0702102104. [PubMed: 17609381]
25. Barnitz RA, Chaigne-Delalande B, Bolton DL, Lenardo MJ. Exposed hydrophobic residues in human immunodeficiency virus type 1 Vpr helix-1 are important for cell cycle arrest and cell death. PLoS ONE. 2011; 6:e24924. doi:10.1371/journal.pone.0024924. [PubMed: 21949789]
26. Doublie S. Preparation of selenomethionyl proteins for phase determination. Methods in enzymology. 1997; 276:523–530. [PubMed: 9048379]
27. Zhao Y, Chapman DA, Jones IM. Improving baculovirus recombination. Nucleic acids research. 2003; 31:E6–6. [PubMed: 12527795]
28. Kabsch W. Integration, scaling, space-group assignment and post-refinement. Acta crystallographica. Section D, Biological crystallography. 2010; 66:133–144. doi:10.1107/S0907444909047374.

29. Sheldrick GM. A short history of SHELX. Acta crystallographica Section A, Foundations of crystallography. 2008; 64:112–122. doi: 10.1107/S0108767307043930.
30. Vonrhein C, Blanc E, Roversi P, Bricogne G. Automated structure solution with autoSHARP. Methods in molecular biology. 2007; 364:215–230. doi:10.1385/1-59745-266-1:215. [PubMed: 17172768]
31. Cowtan K. The Buccaneer software for automated model building. 1. Tracing protein chains. Acta crystallographica. Section D, Biological crystallography. 2006; 62:1002–1011. doi:10.1107/S0907444906022116.
32. Emsley P, Cowtan K. Coot: model-building tools for molecular graphics. Acta Crystallogr D Biol Crystallogr. 2004; 60:2126–2132. [PubMed: 15572765]
33. Afonine PV, et al. Towards automated crystallographic structure refinement with phenix.refine. Acta crystallographica. Section D, Biological crystallography. 2012; 68:352–367. doi:10.1107/S0907444912001308.
34. Krissinel E, Henrick K. Secondary-structure matching (SSM), a new tool for fast protein structure alignment in three dimensions. Acta Crystallogr D Biol Crystallogr. 2004; 60:2256–2268. [PubMed: 15572779]
35. Yap MW, Nisole S, Lynch C, Stoye JP. Trim5alpha protein restricts both HIV-1 and murine leukemia virus. Proc Natl Acad Sci U S A. 2004; 101:10786–10791. [PubMed: 15249690]
36. Bock M, Bishop KN, Towers G, Stoye JP. Use of a transient assay for studying the genetic determinants of Fv1 restriction. J Virol. 2000; 74:7422–7430. [PubMed: 10906195]
37. Groom HC, et al. Absence of xenotropic murine leukaemia virus-related virus in UK patients with chronic fatigue syndrome. Retrovirology. 2010; 7:10. doi: 10.1186/1742-4690-7-10. pii: 1742-4690-7-10. [PubMed: 20156349]
38. Naldini L, et al. In vivo gene delivery and stable transduction of nondividing cells by a lentiviral vector. Science. 1996; 272:263–267. [PubMed: 8602510]
39. Bainbridge JW, et al. In vivo gene transfer to the mouse eye using an HIV-based lentiviral vector; efficient long-term transduction of corneal endothelium and retinal pigment epithelium. Gene therapy. 2001; 8:1665–1668. doi:10.1038/sj.gt.3301574. [PubMed: 11895005]
40. Sundstrom C, Nilsson K. Establishment and characterization of a human histiocytic lymphoma cell line (U-937). International journal of cancer. Journal international du cancer. 1976; 17:565–577. [PubMed: 178611]
41. Gallois-Montbrun S, et al. Antiviral protein APOBEC3G localizes to ribonucleoprotein complexes found in P bodies and stress granules. Journal of virology. 2007; 81:2165–2178. doi:10.1128/JVI.02287-06. [PubMed: 17166910]
42. Negre D, et al. Characterization of novel safe lentiviral vectors derived from simian immunodeficiency virus (SIVmac251) that efficiently transduce mature human dendritic cells. Gene Ther. 2000; 7:1613–1623. doi:10.1038/sj.gt.3301292. [PubMed: 11083469]

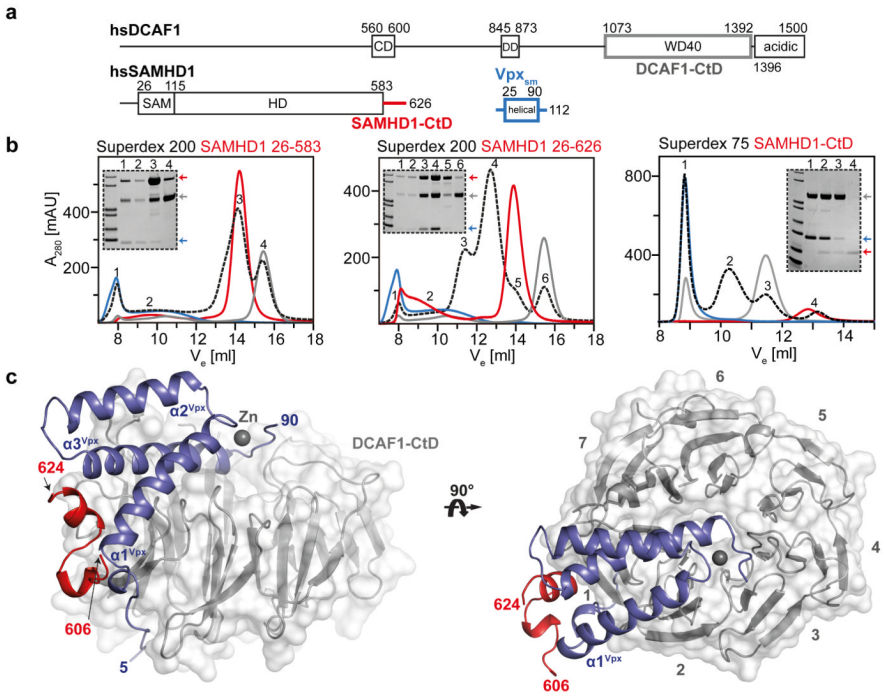

Figure 1. The SAMHD1-CtD/Vpx$_{sm}$/DCAF1-CtD complex

(**a)** Schematic of proteins, CD – chromo domain, DD – dimerisation domain, SAM – sterile alpha motif, HD – His/Asp domain. Regions coloured grey (DCAF1, 1058-1396), red (SAMHD1, 582-626) and blue (Vpx$_{sm}$, 1-112) were used for crystallisation. (**b**) Size exclusion chromatograms (black) of equimolar mixtures of Vpx$_{sm}$, DCAF1-CtD and SAMHD1(26-583) (left), SAMHD1(26-626) (middle) and SAMHD1(582-626) (right). Chromatograms from individual components are also shown Vpx$_{sm}$ (blue), DCAF1-CtD (grey) and SAMHD1 (red). SDS-PAGE analyses of peaks are inset. Peak1 (void volume) contains unspecific aggregates. (**c**) Cartoon representation of the ternary complex. DCAF1-CtD, is shown in grey surface, β-propeller blades are numbered. SAMHD1-CtD is red, Vpx$_{sm}$ is blue and a zinc ion shown as grey sphere.

Europe PMC Funders Author Manuscripts

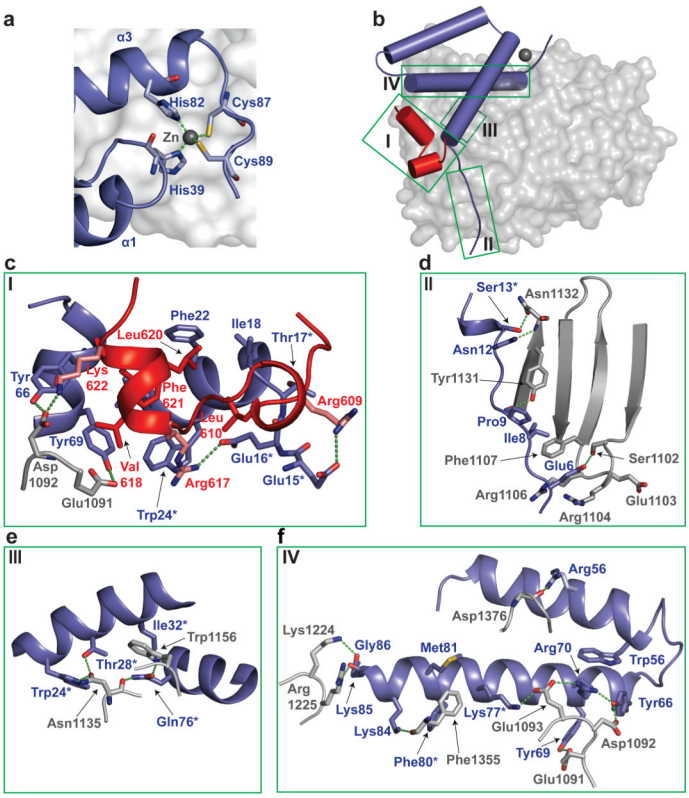

Figure 2. Intermolecular interfaces

(a) Zn ion (grey sphere) and surrounding residues. Co-ordinating residues are displayed as sticks, co-ordinate bonds as green dashes. (**b**) Cartoon representation of SAMHD1-CtD/Vpx_{sm}/DCAF1-CtD. DCAF1-Ctd is shown in grey, cylinders represent α-helices in SAMHD1-CtD (red) and Vpx_{sm} (blue), intermolecular interfaces are highlighted by green boxes (I, II, III, IV). **(c-f)** Views of the interface between SAMHD1-CtD/Vpx_{sm}/DCAF1-CtD (Box I) and Vpx_{sm}/DCAF1-CtD (Box I-IV). Residues contributing to the interface are shown as sticks, hydrogen-bonding interactions as dashed lines and residues important for Vpx function highlighted with an asterisk.

Europe PMC Funders Author Manuscripts

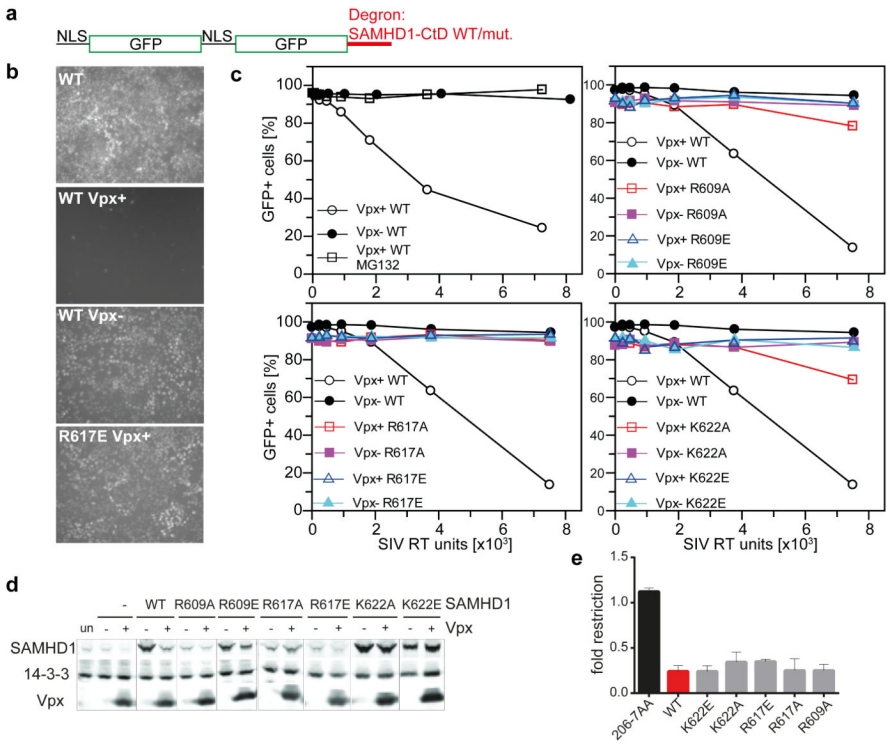

Figure 3. SAMHD1 C-terminal region

(a) The NLS-GFP-SAMHD1-CtD degron. **(b)** Microscopic images of uninfected and SIV Vpx+/− infected 293T cells expressing NLS-GFP-SAMHD1-CtD wildtype or mutant R617E. **(c)** Quantitative analysis of GFPSAMHD1 degron expression following infection with SIV Vpx+/− viruses. Percentages of GFP^+ cells are plotted against SIV virus titre. MG132 was added where indicated. Upper left panel is representative of three independent experiments. **(d)** Immunoblots of 293T cells co-transfected with SAMHD1 and Vpx plasmids (un, untransfected; −, empty vector; +, Vpx) probed with antibodies to SAMHD1 (upper), 14-3-3 (middle) or Vpx_{HIV-2} (lower), representative of two independent experiments. **(e)** Restriction of HIV-1 infection by WT SAMHD1 and mutants. Restriction is expressed as a ratio of HIV-infected SAMHD1-transduced to infected SAMHD1-negative cells (>3 independent experiments with different viral stocks). Error bars show standard deviation.

Europe PMC Funders Author Manuscripts

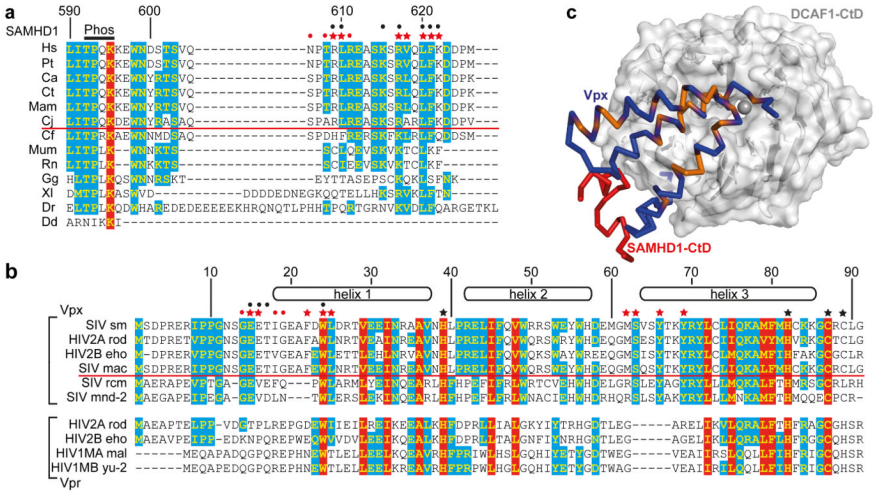

Figure 4. Species specificity of the SAMHD1-Vpx interaction

(**a**) Sequence alignment of the C-termini of SAMHD1. 100% type-conserved residues are boxed red, 60% cyan. Residue numbers refer to hsSAMHD1-CtD. Red stars - side chains involved in Vpx_{sm}-DCAF1-CtD binding, red dots - main chain interactions. Black dots - residues whose mutation impairs DDB1-DCAF1-Vpx binding [8]. Species above the red line are HIV-2/SIV hosts, Phos - phosphorylation site. (**b**) Alignment of Vpx and Vpr proteins, coloured and annotated as in **(a)** numbering refers to Vpx_{sm}. Red stars - side chains involved in SAMHD1-CtD binding, red dots - main chain interactions and black stars - zinc ligands. Black dots indicate residues whose mutation impairs SAMHD1 degradation. Proteins above the red line induce degradation of human SAMHD1, proteins below cannot. (**c**) Type-conserved amino acid residues in Vpx_{sm} and Vpr_{HIV-1} (orange) mapped onto the Vpx_{sm} (blue ribbon)-DCAF1-CtD (white surface) structure. SAMHD1-CtD is shown as red ribbon.

Europe PMC Funders Author Manuscripts